REPORT DOCUMENTATION PAGE

Form Approved
OBM No. 0704-0188

1. AGENCY USE ONLY *(Leave blank)*	2. REPORT DATE	3. REPORT TYPE AND DATES COVERED
	August 1998	Proceedings

4. TITLE AND SUBTITLE

Semi-Automated Maltese Front Position Determination

5. FUNDING NUMBERS

Job Order No.

Program Element No. 0603207N

Project No.

Task No.

Accession No.

6. AUTHOR(S)

Suzanne M. Lea* and Matthew Lybanon

7. PERFORMING ORGANIZATION NAME(S) AND ADDRESS(ES)

Naval Research Laboratory
Oceanography Division
Stennis Space Center, MS 39529-5004

8. PERFORMING ORGANIZATION REPORT NUMBER

NRL/PP/7340--97-0040

9. SPONSORING/MONITORING AGENCY NAME(S) AND ADDRESS(ES)

Office of Naval Research
800 North Quincy Street
Arlington, VA 22217-5000

10. SPONSORING/MONITORING AGENCY REPORT NUMBER

11. SUPPLEMENTARY NOTES

Proceedings of the 14th International Conference on Pattern Recognition, Volume II, 16-20 August 1998, Brisbane, Australia
*Department of Mathematical Sciences, University of North Carolina at Greensboro, NC 27412

12a. DISTRIBUTION/AVAILABILITY STATEMENT

Approved for public release; distribution unlimited.

12b. DISTRIBUTION CODE

13. ABSTRACT *(Maximum 200 words)*

We investigate the reliability of a semi-automated system designed to locate the Maltese front from satellite AVHRR and SAR imagery. The opening and closing operations of mathematical morphology afford a means of image segmentation that provides smooth strong, continuous edges except where the edges are obscured by clouds or similar phenomena. We evaluate the results by comparing them with front positions found by experienced Navy analysts. Our system provides an objective method for front location that is less labor-intensive than manual methods currently in use.

14. SUBJECT TERMS

Maltese front, AVHRR, SAR, satellite imagery, morphology, image segmentation, Gulf Stream, Sicily, Mediterranean Sea, and SST

15. NUMBER OF PAGES

6

16. PRICE CODE

17. SECURITY CLASSIFICATION OF REPORT	18. SECURITY CLASSIFICATION OF THIS PAGE	19. SECURITY CLASSIFICATION OF ABSTRACT	20. LIMITATION OF ABSTRACT
Unclassified	Unclassified	Unclassified	SAR

NSN 7540-01-280-5500

Standard Form 298 (Rev. 2-89)
Prescribed by ANSI Std. Z39-18
298-102

Hosted by

APRS

IAPR

ICPR '98

Proceedings

14th International Conference on Pattern Recognition • Volume II

August 16–20, 1998 • Brisbane, Australia

Sponsored by

CSIRO AUSTRALIA

IIB

Department of Tourism, Small Business and Industry

University of Ballarat

curtin

THE UNIVERSITY OF QUEENSLAND

MONASH
AUSTRALIA'S INTERNATIONAL UNIVERSITY

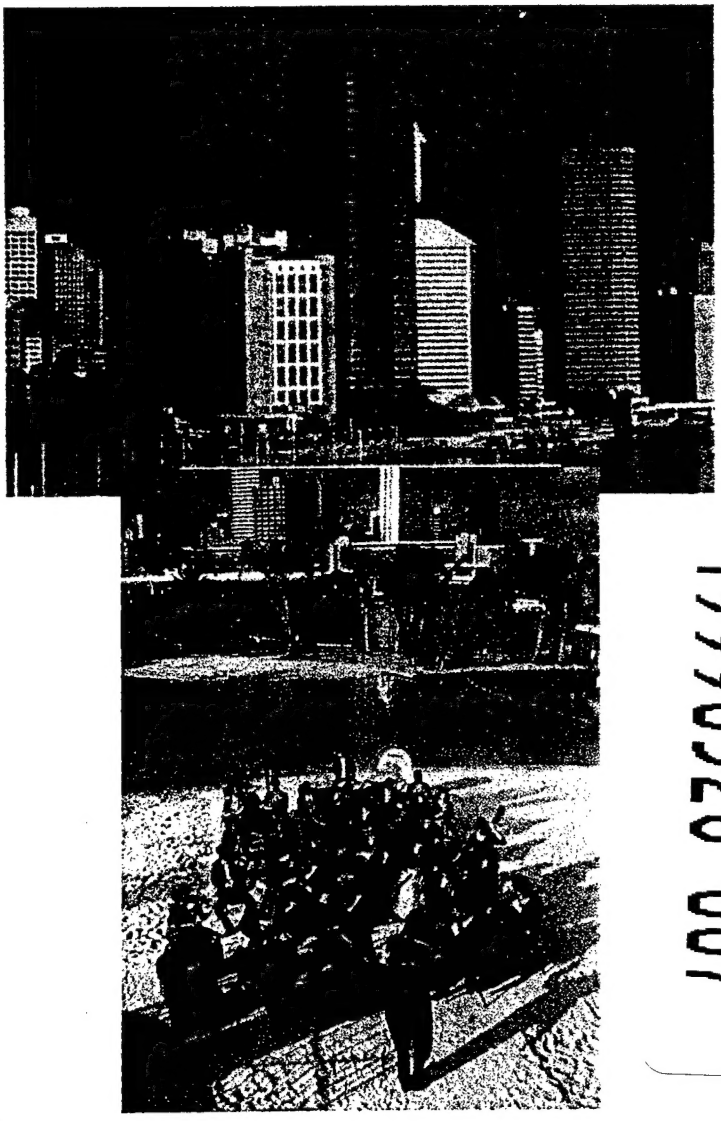

Editors
Anil K. Jain, Svetha Venkatesh, and Brian C. Lovell

IEEE COMPUTER SOCIETY

IEEE

Semi-Automated Maltese Front Position Determination

Suzanne M. Lea
Department of Mathematical Sciences
University of North Carolina at Greensboro
Greensboro, NC 27412
smlea@hamlet.uncg.edu

Matthew Lybanon
Remote Sensing Applications Branch
Naval Research Laboratory
Stennis Space Center, MS 39529-5004
lybanon@snaps.nrlssc.navy.mil

Abstract

We investigate the reliability of a semi-automated system designed to locate the Maltese front from satellite AVHRR and SAR imagery. The opening and closing operations of mathematical morphology afford a means of image segmentation that provides smooth, strong, continuous edges except where the edges are obscured by clouds or similar phenomena. We evaluate the results by comparing them with front positions found by experienced Navy analysts. Our system provides an objective method for front location that is less labor-intensive than manual methods currently in use.

1. Introduction

Oceanic temperature fronts occur where warm and cold water meet. Differences in water temperature, salinity, density, and sea surface roughness show the presence of a temperature front. This work uses sea surface temperature differences and sea surface roughness to locate the surface position of the Maltese front, a boundary separating two water areas near Sicily and Malta that differ in temperature by at most 1.0-1.5°C.

The Maltese front's position varies daily and seasonally. During colder months, it is oriented north-south and located east of Malta and Sicily; in warmer months, it is oriented east-west, and located between Sicily and Malta. In winter, the temperature difference between the two water masses may be less than 0.5°C, and the front's position may not be well-defined in sea surface temperature images. The location of the front is of interest to oceanographers for the information it provides about water motion in the Mediterranean Sea.

This work's purpose was to investigate the reliability of a semi-automated system designed to locate the front. Presently, Navy analysts manually mark the front's daily position as a set of 10-20 geographical points, which can be interpolated by various types of curves. The operation is labor-intensive, subjective and dependent on the skill of the analyst.

Our semi-automated system uses mathematical morphology to find the surface position of the front, and offers the operator a choice among a few of the most likely front positions. The system grew out of previous work on finding the position of the Gulf Stream and associated rings [1, 2], which was successfully extended to the much weaker Maltese front.

2. Images

Fronts are three-dimensional phenomena. Satellite sensors provide only two-dimensional information, although altimeter data indirectly provides information about subsurface structure. Oceanographers modeling a front match a feature model to the satellite data at the surface and infer subsurface features from model predictions [3, 4, 5].

The sea surface temperature (SST) images used in this study are products of the NOAA-11 satellite's AVHRR (Advanced Very High Resolution Radiometer). The data from two AVHRR channels is combined to calculate a sea surface temperature (intensity) in °C to the closest 0.1°C; the accuracy of the temperatures is 0.5 to 1.0°C [6].

Synthetic aperture radar (SAR) images from the ERS-1 satellite provide information on sea surface roughness. High-intensity areas in SAR images correspond to areas that reflect radar well, which are qualitatively rougher than surrounding (lower-intensity) smooth areas.

3. Analysis and results

In both sets of images, the front boundary corresponds to an edge separating two water masses with different intensity values. Finding the location of the front requires finding the largest temperature value (T_f) or roughness value (R_f) corresponding to pixels on the cold or less

rough side of the front. The system then smoothes the temperature or roughness values in the image and zeroes all pixels with temperature or roughness less than or equal to T_f (R_f). The boundary between zero and nonzero pixels represents the desired front location.

Since the images are 1 byte/pixel images, the semi-automated system (or human analyst) initially has 256 choices for T_f. The system is designed to use image information to reduce the number of choices to one or a few, among which is the correct value.

Mathematical morphology [7, 8, 9] has been used successfully to find front positions in ocean images [1, 2]. The opening and closing operations of mathematical morphology, based on the familiar dilation and erosion operators, perform intensity smoothing that results in smoothing of edges. Consequently, these operators are an excellent choice for image segmentation where edges are ultimately to be found; they provide smooth, strong, continuous edges except where the edges are obscured by clouds or similar phenomena.

3.1. SST images

We used 49 SST images of the Mediterranean Sea, acquired between March and September 1993, in constructing the semi-automated system. These images are 2048×1024×16 bits, covering the entire Mediterranean Sea (29.6°-42.0° North latitude, 7.0°-37.7° East longitude). Preprocessing extracted the Sicily-Malta area (34.04°-37.16° North latitude, 13.36°-17.18° East longitude) and the temperature range considered (7.5°C-33.0°C) while preserving the original temperature resolution. This range includes all surface water temperatures likely to be observed in the Sicily-Malta area of the Mediterranean Sea.

The semi-automated system uses three image parameters, predicted mean temperature T_p, image quality Q, and predicted maximum front temperature T_f, calculated from image statistics: temperature minimum, maximum, mean, and standard deviation (σ).

A good fit to the mean temperatures of the 49 images is provided by a single frequency sinusoid (Fig. 1),

$$T_p = 134.07 - 70.71 \sin(2\pi(d - 36.68)/365), \qquad (1)$$

where d is the ordinal number of the day in the year. The curve parameters are derived from a least-squares fit to the means of the 25 best images, selected based on visual observation and the hypothesis that good images have higher means than poor images (those with clouds or missing data) of close to the same date. The x^2 value for the fit is 3.00 for 22 degrees of freedom. Maximum and minimum values occur respectively on August 25 and February 24; these values agree well with seasonal lag and the ocean surface water minimum and maximum temperature dates [10]. Eq. (1) does not necessarily predict water temperature; cold clouds may unduly bias March data, and hot land September data.

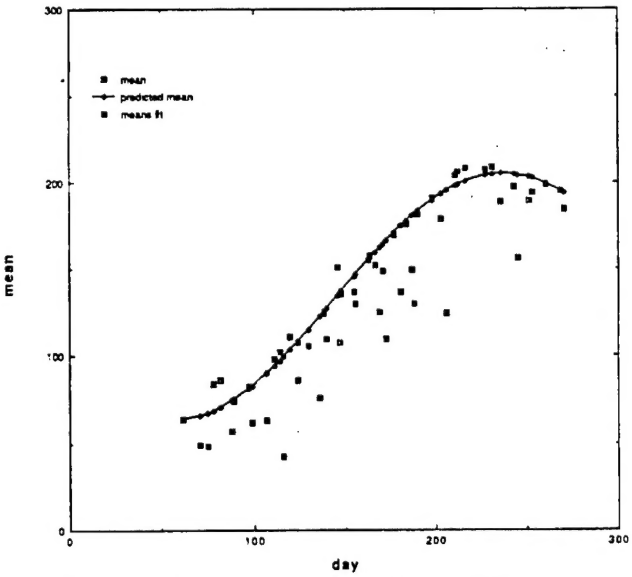

Figure 1. Mean temperature for SST images (after preprocessing) as a function of day in the year. The curve is a single frequency sinusoid fit to the means of the 25 best images.

Clouds covering the front indicate a poor quality image; they lower the mean temperature below the predicted mean and cause an extended low-temperature tail in the image histogram. A combination of these effects was selected to define image quality:

$$Q = (|T_p - T_{mean}| + \sigma) / T_{mean}. \qquad (2)$$

A good image has $Q < 0.5$, a value selected based on visual observation of image quality.

We also used visual inspection to find a predicted T_f value. We found values for good and poor images and made separate least-squares fits. The fits are not outstanding, particularly in good images, where outlying points affect the x^2 value excessively, but they provide a reasonable starting point for the system. The fits used are:

$$T_f = 0.95\, T_{mean} + 0.13\,(T_p - T_{mean}) - 0.42 \qquad \text{(good)}$$
$$T_f = 0.72\, T_{mean} + 0.77\,\sigma + 4.7 \qquad \text{(poor).}$$

The x^2 values are respectively 7.06 (good, 35 degrees of freedom) and 0.06 (poor, 12 degrees of freedom). Good

images have $T_f < T_{mean}$, whereas poor images have $T_f > T_{mean}$.

Parameters required by mathematical morphology are a structuring element size, selected as 3 × 3, and a starting threshold, selected as *min* $(T_f - 2.4, T_{mean} - 1.0)$ in °C, though it may be any value lower than T_f. Once the parameters are specified, the opening and closing operations are performed at threshold intensities increasing by 1 each iteration, and the number of image pixels that change classification from background to object or vice versa is found for each iteration. An edge corresponds to a threshold value where the fewest pixels change classification, that is, to a sudden intensity jump.

The number of pixels changing classification fluctuates rapidly from one intensity value to the next. We use a sliding window to accumulate total changes in bin sizes of 3 (0.3°C intensity edge) through 5 (0.5°C edge) intensity values. We then combine overlapping minima and add a bin that starts on the correct side of the mean (according to the image quality prediction) and ends at the mean. The identification of bins containing minima continues until either at least two bins are found, with one that contains the T_f value, or minima with bin size 3 are exhausted. The temperature corresponding to the minimum number of changes in a bin is chosen as the T value for that bin.

Our semi-automated system sorts bins found based on the likelihood that each minimum contains the front, using the following criteria:

(1) A minimum on the incorrect side of the mean (as judged by image quality) cannot be the actual front and is eliminated.

(2) The bin (if any) that contains the predicted T_f value is the most likely one to contain the front and is listed first. If the predicted T_f value is not in any bin, a bin extending from the minimum below the predicted value to the minimum above it is added, with the predicted value as the T value for the bin.

(3) Larger bins (temperature differences) are more likely to be the actual front than smaller bins.

(4) Bins closer to the predicted T_f value are preferred to those further from it.

The bins found are identical to those selected by a human analyst. On the average, 2.9 bins are found for each image; the smallest number found is 1, and the largest, 6.

The system displays the original image and up to 5 segmented images:

(1) If the predicted T_f value is in a bin, the T values for the first four bins found are sorted in order of likelihood and displayed. If the system finds fewer than four bins, it displays fewer.

(2) If the predicted T_f value is not in a bin, the T values for the first three bins found are sorted in order of likelihood and are displayed with the predicted value. If the system finds fewer than three bins, it displays fewer.

The user may choose to accept a displayed image as accurately locating the front (and save it), to explore other possible T values in a bin, or to select an arbitrary T_f value and segment using it, causing display of a fifth segmented image.

The four or fewer segmented images chosen for display contain the observed T_f value for 48 of the 49 test images (98%). The exception is a poor-quality image for which the predicted T_f value is quite uncertain and where no value gives a reasonable location for the Maltese front. The observed T_f value is the program's first choice for only 31 of the 49 images (63%), but since it is a semi-automated system it has the advantage that the operator can overrule it when necessary, while the program does most of the work in finding the front.

Figure 2. 30 July 1993 SST image of the Maltese front area with fronts found using mathematical morphology (solid line) and NAVOCEANO daily analysis (dashed line) superimposed. The grid is East longitude and North latitude.

The quality of the resulting front positions is judged by comparison with the front position found by experienced Navy analysts. Fig. 2 shows the semi-automated and human-analyst fronts superimposed on an original SST image. Error is estimated by finding the area between the

fronts and dividing the are by the arclength of the human-defined front, giving a mean error in front position expressed in km. The mean error for the 49 images is 10.05 km, with standard deviation 5.40 km and range 4.02 km to 28.64 km [11].

3.2. SAR images

We used six SAR images of the Mediterranean Sea, acquired between March an September 1993, to compare front location using temperature with front location using sea surface roughness. These images are approximately 8000×8000×16 bits, covering the area where the Maltese front is located. The images were made on dates close to those of six SST images. Preprocessing averaged neighborhoods of 8×8 pixels to reduce variations in roughness caused by waves, rotated the images to geographical coordinates, and removed the gradient caused by variable detector distances by dividing by a gradient image.

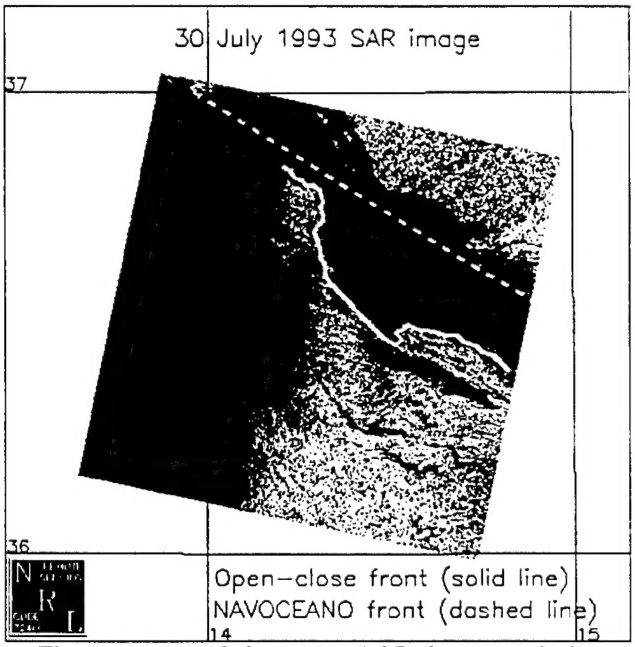

Figure 3. 30 July 1993 SAR image of the Maltese front area with fronts found using mathematical morphology (solid line) and NAVOCEANO daily analysis (dashed line) superimposed. The grid is East longitude and North latitude.

Fronts in SAR images appear as transitions from low to high surface roughness. Both temperature and wind fronts are evident in the images; wind fronts are better defined (sharper) than temperature fronts. We used mathematical morphology to extract front positions in these images as well. For the SAR images, since temperature fronts are noisier than wind fronts, the most likely roughness R_f (corresponding to T_f in SST images) occurs when the most pixels are changing classification. There is a single clear maximum in each SAR image tested, with a value of R_f that yields a front position agreeing moderately well with that found by the human analyst in SST images. Unfortunately, wind fronts (when present) have R_f values less than the R_f for the temperature front, and are found also. The human analyst must distinguish the two.

Fig. 3 shows the semi-automated and human-analyst fronts superimposed on an original SAR image. The roughness and temperature positions are close but not identical. Wind may affect the roughness front position. (Note that Fig. 3 and Fig. 2 use different scales.) Fig. 4 shows the semi-automated fronts from SST and SAR images of the same date, and the front located by the human analyst, superimposed on an original SST image.

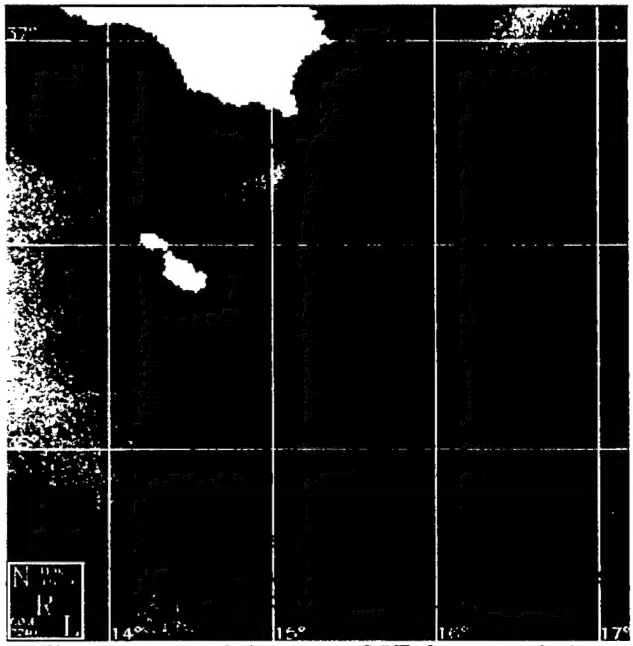

Figure 4. 30 July 1993 SST image of the Maltese front area with fronts found using mathematical morphology from SST image (solid line) and from SAR image (dash-dotted line), and front from NAOVOCEANO daily analysis (dashed line) superimposed. The grid is East longitude and North latitude.

4. Conclusions

The semi-automated system produces Maltese front surface positions that agree well with those found by experienced human analysts in 48 of 49 test images

(98%). It takes advantage of simple image statistics to produce 2 to 4 candidate front positions rapidly, allowing the operator to use experience with the front's surface position at various times of the year to select the best candidate from among those offered, or to overrule the system and select a position based entirely on experience. Our system provides an objective method of locating fronts that is less labor-intensive than manual methods currently in use.

References

[1] S. M. Lea and M. Lybanon. Finding mesoscale ocean structures with mathematical morphology. *Rem. Sens. Environ.*, 27(1):46-56, 1993.

[2] S. M. Lea and M. Lybanon. Automated boundary delineation in infrared ocean images. *IEEE Trans. Geosci. and Rem. Sens.*, 31(6):1256-1260, Nov. 1993.

[3] T. J. Bennett, Jr., M. R. Carnes, P. A. Phoebus, and L. M. Riedlinger. Feature modeling: the incorporation of a front and eddy map into optimum interpolation-based thermal analyses. *NORDA Rept. 242*, Naval Research Laboratory, Stennis Space Center, MS, 1989.

[4] S. M. Glenn, G. Z. Forristall, P. Cornillon, and G. Milkowski. Observations of Gulf Stream ring 83-E and their interpretation using feature models. *J. Geophys. Res.*, 95:13043-13063, 1990.

[5] A. R. Robinson and L. J. Walstad. The Harvard open ocean model: calibration and application to dynamical processes, forecasting, and data assimilation studies. *Applied Numerical Math.*, 3:89-131, 1987.

[6] E. P. McLain, W. G. Pichel, and C. C. Walton. Comparative performance of AVHRR-based multichannel sea surface temperatures. *J. Geophys. Res.*, 90(C6):11587-11601, 1985.

[7] J. Serra. *Image Analysis and Mathematical Morphology*. Academic Press, New York, NY, 1982.

[8] R. M. Haralick, S. R. Sternberg, and X. Zhuang. Image analysis using mathematical morphology. *IEEE Trans. Pattern Anal. and Machine Intell.*, PAMI-9(4):532-550, July 1987.

[9] S. R. Sternberg. Grayscale morphology. *Comp. Vis., Graphics, and Image Proc.*, 35(3):333-355, Sept. 1986.

[10] H. U. Sverdrup, M. W. Johnson, and R. H. Fleming. *The Oceans: Their Physics, Chemistry, and General Biology*. Prentice-Hall, Englewood Cliffs, NJ, 1942.

[11] M. Lybanon. Maltese front variability from satellite observations based on automated detection. *IEEE Trans. on Geosci. and Rem. Sens.*, 34(5):1159-1165, Sept. 1996.

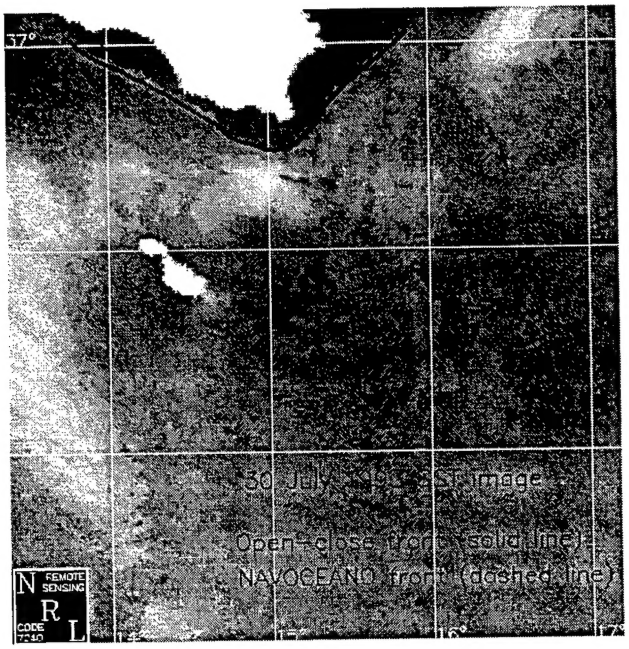

Figure 2: July 30, 1993, SST image of the Maltese front area with fronts found using mathematical morphology (solid line) and NAVOCEANO daily analysis (dashed line) superimposed. The grid is East longitude and North latitude.

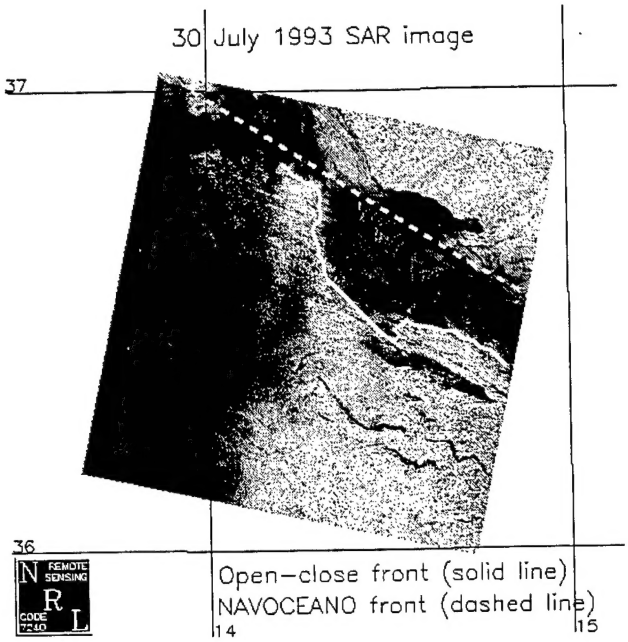

Figure 3: July 30, 1993, SAR image of the Maltese front area with fronts found using mathematical morphology (solid line) and NAVOCEANO daily analysis (dashed line) superimposed. The grid is East longitude and North latitude.

3.2 SAR images

We used six SAR images of the Mediterranean Sea, acquired between March and September 1993, to compare front location using temperature with front location using sea surface roughness. These images are approximately 8000 × 8000 × 16 bits, covering the area where the Maltese front is located. The images were made on dates close to those of six SST images. Preprocessing averaged neighborhoods of 8 × 8 pixels to reduce variations in roughness caused by waves, rotated the images to geographical coordinates, and removed the gradient caused by variable detector distances by dividing by a gradient image.

Fronts in SAR images appear as transitions from low to high surface roughness. Both temperature and wind fronts are evident in the images; wind fronts are better defined (sharper) than temperature fronts. We used mathematical morphology to extract front positions in these images as well. For the SAR images, since temperature fronts are noisier than wind fronts, the most likely roughness R_f (corresponding to T_f in SST images) occurs when the most pixels are changing classification. There is a single clear maximum in each SAR image tested, with a value of R_f that yields a front position agreeing moderately well with that found by the human analyst in SST images. Unfortunately, wind fronts (when present) have R_f values less than the R_f for the temperature front, and are found also. The human analyst must distinguish the two.

Fig. 3 shows the semi-automated and human analyst fronts superimposed on an original SAR image. The roughness and temperature positions are close but not identical. Wind may affect the roughness front position. (Note that Fig. 3 and Fig. 2 use different scales.) Fig. 4 shows the semi-automated fronts from SST and SAR images of the same date, and the front located by the human analyst, superimposed on an original SST image.

4 Conclusions

The semi-automated system produces Maltese front surface positions that agree well with those found by experienced human analysts in 48 of 49 test images (98%). It takes advantage of simple image statistics to produce 2 to 4 candidate front positions rapidly, allowing the operator to use experience with the front's surface position at various times of the year to select the best candidate from among those offered, or to overrule the system and select a position based entirely on experience. Our system provides an objective method of locating fronts that is less labor-intensive than manual

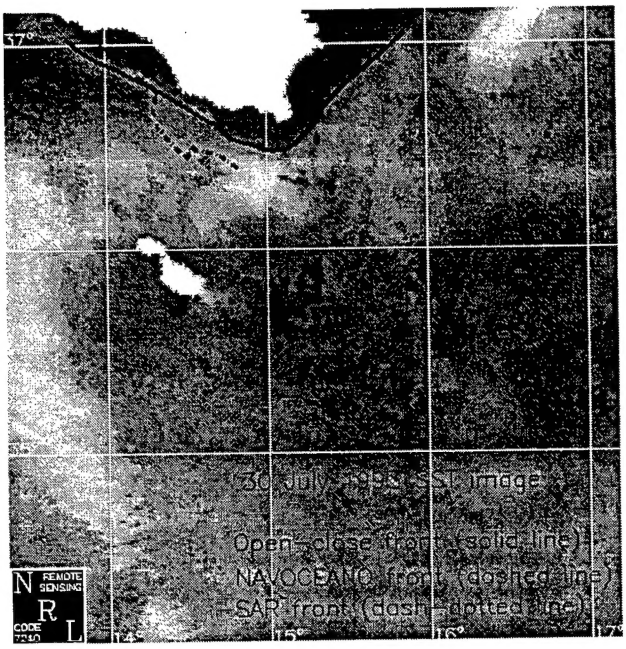

Figure 4: July 30, 1993, SST image of the Maltese front area with fronts found using mathematical morphology from SST image (solid line) and from SAR image (dash-dotted line), and front from NAOVOCEANO daily analysis (dashed line) superimposed. The grid is East longitude and North latitude.

methods currently in use.

References

[1] S. M. Lea and M. Lybanon. Finding mesoscale ocean structures with mathematical morphology. *Rem. Sens. Environ.*, **27**(1):46-56, 1993.

[2] S. M. Lea and M. Lybanon. Automated boundary delineation in infrared ocean images. *IEEE Trans. Geosci. and Rem. Sens.*, **31**(6):1256-1260, Nov. 1993.

[3] T. J. Bennett, Jr., M. R. Carnes, P. A. Phoebus, and L. M. Riedlinger. Feature modeling: the incorporation of a front and eddy map into optimum interpolation-based thermal analyses. Naval Research Laboratory, Stennis Space Center, MS, NORDA Rept. 242, 1989.

[4] S. M. Glenn, G. Z. Forristall, P. Cornillon, and G. Milkowski. Observations of Gulf Stream ring 83-E and their interpretation using feature models. J. *Geophys. Res.*, **95**:13043-13063, 1990.

[5] A. R. Robinson and L. J. Walstad. The Harvard open ocean model: calibration and application to dynamical processes, forecasting, and data assimilation studies. *Applied Numerical Math.*, **3**:89-131, 1987.

[6] E. P. McLain, W. G. Pichel, and C.C. Walton. Comparative performance of AVHRR-based multichannel sea surface temperatures. *J. Geophys. Res.*, **90**(C6):11587-11601, 1985.

[7] J. Serra. *Image Analysis and Mathematical Morphology.* Academic Press, New York, NY, 1982.

[8] R. M. Haralick, S. R. Sternberg, and X. Zhuang. Image analysis using mathematical morphology. *IEEE Trans. Pattern Anal. and Machine Intell.*, **PAMI-9**(4):532-550, July 1987.

[9] S. R. Sternberg. Grayscale morphology. *Comp. Vis., Graphics, and Image Proc.*, **35**(3):333-355, Sept. 1986.

[10] H. U. Sverdrup, M. W. Johnson, and R. H. Fleming. *The Oceans: Their Physics, Chemistry, and General Biology.* Prentice-Hall, Englewood Cliffs, NJ, 1942.

[11] M. Lybanon. Maltese front variability from satellite observations based on automated detection. *IEEE Trans. on Geosci. and Rem. Sens.*, **34**(5):1159-1165, Sept. 1996.